Origins of the Zigzag Scan in Transform-Based Picture Coding

Yuriy A. Reznik
Brightcove, Inc. (USA)

ABSTRACT

We review the history of the development of one of the most iconic tools in image and video coding – the zigzag scan. Despite its simplicity, we will show that its development was a non-trivial process that took several years, multiple iterations, and multiple ideas that eventually led to the formation of its final "zigzag" shape. Remarkably, we also discover that early variants of the zigzag scan appeared before the invention of the DCT, intra-predictors, and many other techniques in image and video coding algorithms. It is one of the oldest and most fundamental techniques in this context. This paper also traces the evolution of image and video codec architectures over the last six decades and brings examples of uses of the zigzag scan in modern-era image and video coding standards.

Keywords: Image and video coding, Fourier analysis, Boas-Kac-Lukosz inequalities, DFT, DCT, KLT, zigzag scan.

1. INTRODUCTION

Digital image and video coding have a long and illustrious history. Some milestones, such as the invention of the Discrete Cosine Transform (DCT) and the first image and video compression standards (H.261, JPEG, MPEG-1, MPEG-2, etc.), are well known. Many books and papers describe them in detail. However, the invention of the zigzag scan seems to have escaped due attention. Modern books do not say much about it. It is puzzling, considering that the zigzag scan order has been present in almost every DCT-based image and video compression standard since H.261 and JPEG (cf. Figure 1).

Who originally invented it, and for what purpose?

In this paper, we will try to answer these questions. On this quest, we will survey many early image and video coding papers and try to find developments leading to the formation of the zigzag scan. We will try to understand the original motivations for this technique, its initial implementations, and convergence towards its final "zigzag" shape. We will also trace the evolution of image codec architectures, leading to modern DCT- and multi-transform-based designs. Finally, we will survey the use of the zigzag scan and its variants in H.261, JPEG, CMTT 723, MPEG 1/2, H.264/AVC, JPEG-XR, HEVC, VVC, and other image and video coding standards.

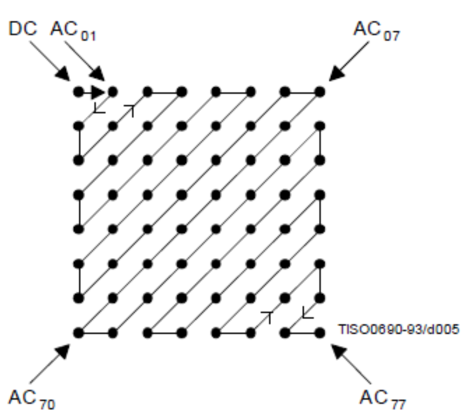

(a)

1	2	6	7	15	16	28	29
3	5	8	14	17	27	30	43
4	9	13	18	26	31	42	44
10	12	19	25	32	41	45	54
11	20	24	33	40	46	53	55
21	23	34	39	47	52	56	61
22	35	38	48	51	57	60	62
36	37	49	50	58	59	63	64

→ Increasing cycles per picture width

↓ Increasing cycles per picture height

(b)

Figure 1. Zigzag scan order for 8x8 blocks as defined in (a) JPEG [1] and (b) H.261 [2] coding standards.

2. THE ORIGINS OF THE ZIGZAG SCAN

2.1. First transform-based image codecs

Reviewing classic image- and video-compression literature [2-31], we discover references to several transform-based image coding algorithms developed in the late 1960s [14-22,26,27]. Among the earliest, we find the designs by Harry C. Andrews and William K. Pratt from the University of Southern California, LA [14-16]. We reproduce the front page of one of these early papers [16] in Figure 2.

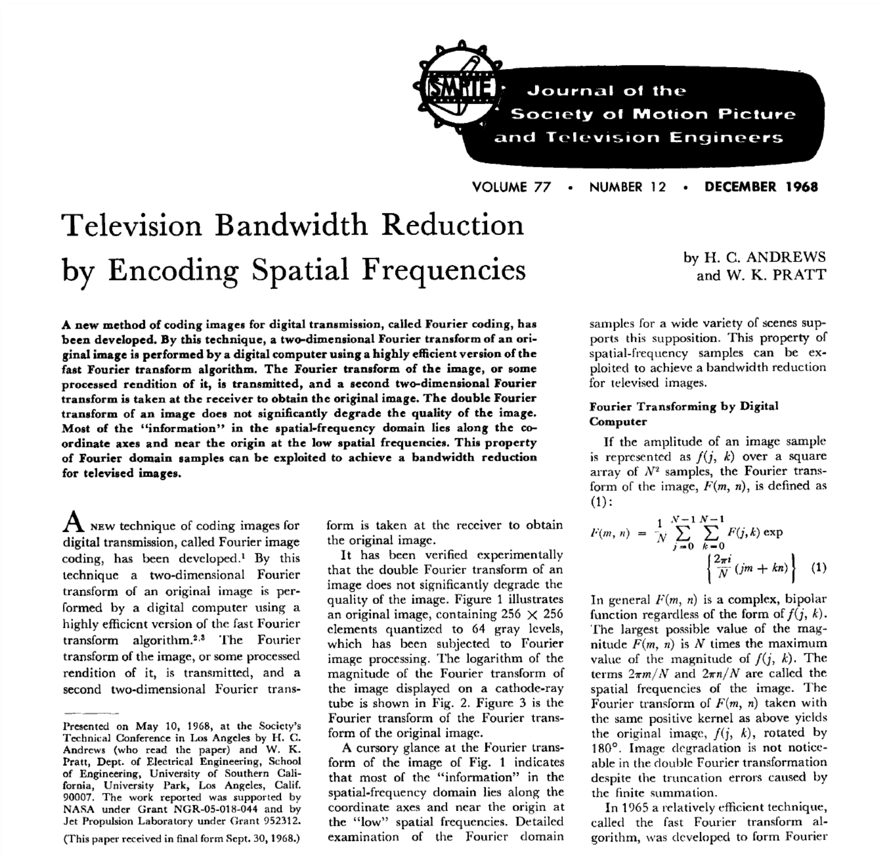

Journal of the Society of Motion Picture and Television Engineers

VOLUME 77 • NUMBER 12 • DECEMBER 1968

Television Bandwidth Reduction by Encoding Spatial Frequencies

by H. C. ANDREWS and W. K. PRATT

A new method of coding images for digital transmission, called Fourier coding, has been developed. By this technique, a two-dimensional Fourier transform of an original image is performed by a digital computer using a highly efficient version of the fast Fourier transform algorithm. The Fourier transform of the image, or some processed rendition of it, is transmitted, and a second two-dimensional Fourier transform is taken at the receiver to obtain the original image. The double Fourier transform of an image does not significantly degrade the quality of the image. Most of the "information" in the spatial-frequency domain lies along the coordinate axes and near the origin at the low spatial frequencies. This property of Fourier domain samples can be exploited to achieve a bandwidth reduction for televised images.

A NEW technique of coding images for digital transmission, called Fourier image coding, has been developed.[1] By this technique a two-dimensional Fourier transform of an original image is performed by a digital computer using a highly efficient version of the fast Fourier transform algorithm.[2,3] The Fourier transform of the image, or some processed rendition of it, is transmitted, and a second two-dimensional Fourier transform is taken at the receiver to obtain the original image.

It has been verified experimentally that the double Fourier transform of an image does not significantly degrade the quality of the image. Figure 1 illustrates an original image, containing 256 × 256 elements quantized to 64 gray levels, which has been subjected to Fourier image processing. The logarithm of the magnitude of the Fourier transform of the image displayed on a cathode-ray tube is shown in Fig. 2. Figure 3 is the Fourier transform of the Fourier transform of the original image.

A cursory glance at the Fourier transform of the image of Fig. 1 indicates that most of the "information" in the spatial-frequency domain lies along the coordinate axes and near the origin at the "low" spatial frequencies. Detailed examination of the Fourier domain samples for a wide variety of scenes supports this supposition. This property of spatial-frequency samples can be exploited to achieve a bandwidth reduction for televised images.

Fourier Transforming by Digital Computer

If the amplitude of an image sample is represented as $f(j, k)$ over a square array of N^2 samples, the Fourier transform of the image, $F(m, n)$, is defined as (1):

$$F(m, n) = \frac{1}{N} \sum_{j=0}^{N-1} \sum_{k=0}^{N-1} F(j,k) \exp \left\{ \frac{2\pi i}{N} (jm + kn) \right\} \quad (1)$$

In general $F(m, n)$ is a complex, bipolar function regardless of the form of $f(j, k)$. The largest possible value of the magnitude $F(m, n)$ is N times the maximum value of the magnitude of $f(j, k)$. The terms $2\pi m/N$ and $2\pi n/N$ are called the spatial frequencies of the image. The Fourier transform of $F(m, n)$ taken with the same positive kernel as above yields the original image, $f(j, k)$, rotated by 180°. Image degradation is not noticeable in the double Fourier transformation despite the truncation errors caused by the finite summation.

In 1965 a relatively efficient technique, called the fast Fourier transform algorithm, was developed to form Fourier

Presented on May 10, 1968, at the Society's Technical Conference in Los Angeles by H. C. Andrews (who read the paper) and W. K. Pratt, Dept. of Electrical Engineering, School of Engineering, University of Southern California, University Park, Los Angeles, Calif. 90007. The work reported was supported by NASA under Grant NGR-05-018-044 and by Jet Propulsion Laboratory under Grant 952312.

(This paper received in final form Sept. 30, 1968.)

Figure 2. Front page from H. C. Andrews and W. K. Pratt's paper [16]. © SMPTE, 1968.

The fundamental operation in Andrews-Pratt encoders was the two-dimensional Fourier transform. The choice of Fourier transform was not coincidental. It was a classic transform with the first fast algorithm recently invented (Cooley-Tookey's FFT [48,49]). The discovery of FFT was a significant factor at that time [50,51].

Figures 3 and 4 illustrate the principles of operation of these early codecs.

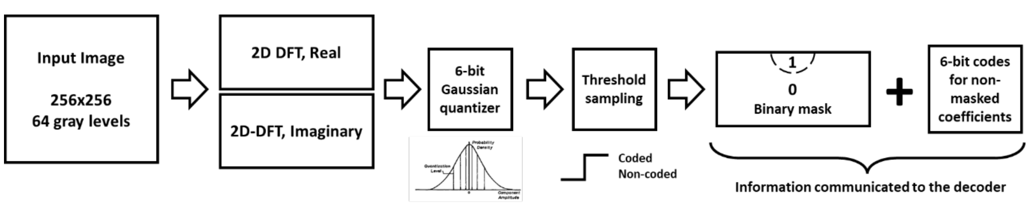

Figure 3. Main processing steps in Andrews-Pratt encoder [16].

As shown in Figure 3, the input to the encoding algorithm is a 256x256-pixel, 6-bit (64-level-quantized) gray-scale image. The first step is the 2D transform. It is applied to an entire image. Due to the conjugate symmetry of the spectra of real inputs, only half of the spectral samples are retained. Hence, the total number of samples in the Fourier domain (including real and imaginary parts) is the same as in the input image. Subsequently, a 6-bit non-uniform quantizer (optimized for Gaussian distribution and fixed-length coding) is applied. According to Andrews and Pratt [16], this choice of the quantizer's granularity and shape allows the reconstruction image to look almost as good as the original. Subsequently, the so-called "binary-mask" technique is applied to reduce the bandwidth. Only coefficients with magnitude values surpassing a particular threshold are transmitted. The binary mask marking the positions of the transmitted coefficients is also communicated to the decoder.

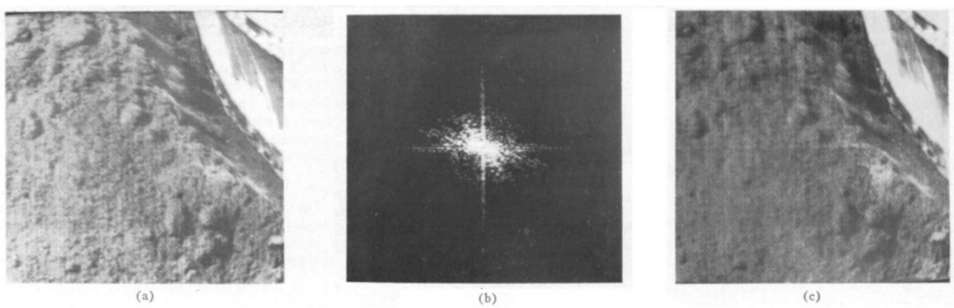

Figure 4. Illustration of operation Andrews-Pratt encoders. (a) The original image. (b) Logarithm magnitude of the Fourier spectrum. (c) The reconstructed image after applying the inverse transform. Reproduced from [18].

The reason why this codec works is evident from Figure 4. The Fourier transform condenses the signal's energy to a few coefficients around the zero-frequency point. Only those few coefficients need to be transmitted. According to [16], this technique reduced the bandwidth by a factor of 4. Considering that input images were 6-bit PCM sampled, this codec operated at 1.5 bits/pixel. A remarkable achievement for an algorithm developed in 1968!

2.2. "Threshold sampling" and "Zonal sampling" methods

Following the original publications [14-16], several variants of Fourier-domain coding techniques have been developed. Among them, we must note:

- "Threshold sampling" methods – selection of samples that surpass a certain threshold in magnitude,
- "Zonal sampling" methods – selection of samples in a pre-defined geometric region on the spectral plane [18].

Pratt and Andrews [18] explain these methods as follows: "In zonal sampling, only those transform samples that lie within certain geometric regions in the transform domain are selected for transmission. The basic problem with zonal sampling is that in certain pictures, many large-magnitude samples may lie outside the zonal region and will, therefore, not be transmitted. In order to avoid such errors, it is possible to establish a threshold level on the magnitude of transform domain samples such that if the transform sample magnitude is greater than the threshold, it will be selected, and the sample will be deleted if it falls below the threshold. With threshold coding it is necessary to code the location in the transform domain of a selected sample as well as its value."

Based on this description, the original "binary mask" method [16] was a variant of a threshold sampling technique. The binary mask marks the locations of the transmitted coefficients. With the "zonal sampling" method, the mask becomes parametrically defined, e.g., as shown in Figure 5.

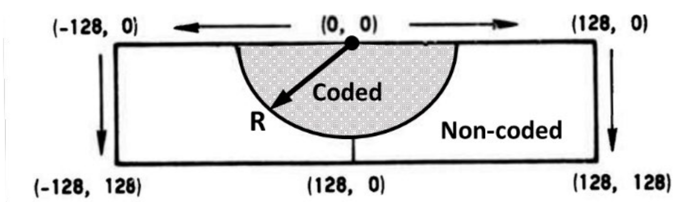

Figure 5. Circular zonal mask for Fourier spectra. A single parameter, R, defines the coded region.

However, when the mask is known, the coefficients' transmission order does not affect compression efficiency. Any order works as long as the decoder follows the same order. In other words, threshold sampling and zonal mask techniques do not yet dictate any particular order for coding and transmission of the coefficients.

In their original paper [16], Andrews and Pratt also mention the possibility of designing a more advanced masking method, avoiding explicit mask transmission. As an idea, they suggest that the quantized Fourier coefficients may be *ordered according to their magnitudes*, and then only the top few transmitted, as allowed by the channel rate. However, they don't explain how to signal such a reordering pattern to the decoder.

2.3. Adaptive coding of Fourier spectra. Lukosz bound. 2D Scan order.

One of the earliest image codecs with *explicitly defined scan orders* appears in the Ph.D. thesis by Andrew G. Tescher [33]. It was presented and defended at the USC in 1973. It was also published as USC research report [34].

A key factor that motivated A. G. Tescher's study was a property of Fourier spectra of non-negative band-limited signals, known as Lukosz bound [52]. In mathematics, it is also known as Boas-Kac inequality [53] (see also [54,55]). In essence, if we have an integrable function $f(t) \geq 0, t \in \mathbb{R}$, with Fourier spectrum

$$F(\omega) = \int_{-\infty}^{\infty} e^{iux} f(t)\, dx, \qquad \omega \in \mathbb{R}, \tag{1}$$

and we require it to be band-limited: $|F(\omega)| = 0,\ |\omega| \geq 1$, then Lukosz bound states that

$$|F(\omega)| \leq F(0)\, \cos\left(\frac{\pi}{\lceil 1/|\omega| \rceil + 1}\right), \quad \omega \in \mathbb{R}. \tag{2}$$

We illustrate the spectral envelope shape implied by the Lukosz bound in Figure 6(a).

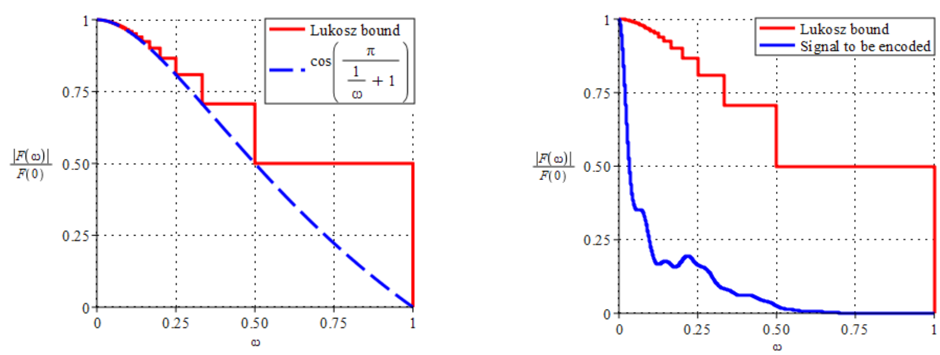

(a) (b)

Figure 6. (a) Lukosz bound construction. (b) Lukosz bound vs. magnitude spectrum of an example non-negative signal.

As evident, the Lukosz bound is immediately helpful for compression. It shows that amplitudes of higher frequencies can be encoded with fewer bits. It also shows that the magnitude of the Fourier spectrum should be more compressible than its phase (the central thesis studied in [33]). However, this bound is conservative. As shown in Figure 6(b), the magnitude spectra of natural signals may decay more rapidly!

This observation leads to the second key idea introduced in A. G. Tescher's work: *encode amplitudes of the Fourier spectrum adaptively*. Send the DC amplitude first, and then, for each subsequent higher-frequency sample, try to predict its variance based on values of previously processed samples. Once the variance of a distribution is known (or estimated by some predictive technique), one can design a quantizer and encode the sample. The adaptive encoding process moves from DC towards Nyquist frequency. Or, as we have noted from Figure 6, in the direction of a *progressive descent along the Lukosz envelope*.

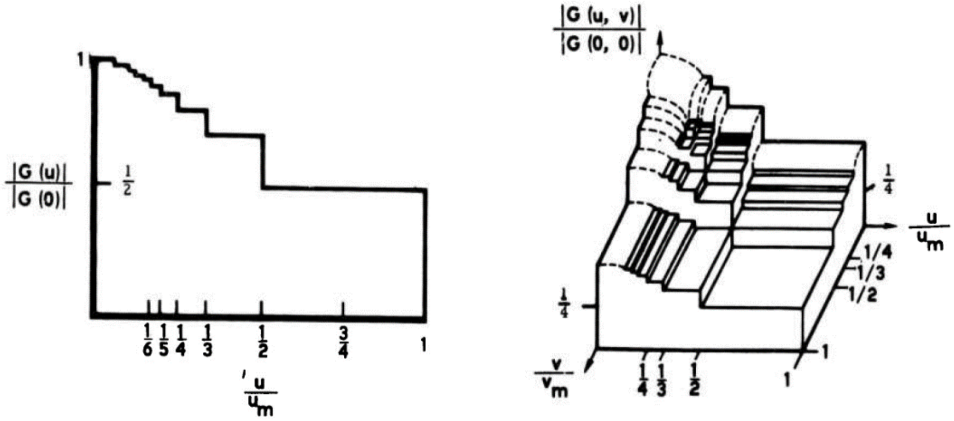

Figure 7. Illustration of application of Lukosz bound to 2D amplitude Fourier spectrum. Reproduced from [33].

In application to images, this idea requires one more twist. Images are two-dimensional signals. As shown in Figure 7, Lukosz bound turns into a 2D surface, simultaneously decaying in horizontal and vertical dimensions. Hence, to implement adaptive coding of spectral coefficients, one must find *a way to walk over this surface, producing a sequence of points with progressively descending magnitudes*.

This observation is the fundamental idea leading to the concept of an optimal scan order. Since the Lukosz bound holds for all images, *only one (universally defined) scan order is required!*

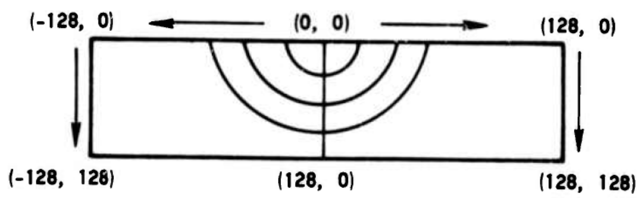

Figure 8. The arrangement of Fourier coefficients of 256x256 image, discarding the upper part due to conjugate symmetry property. Point (0,0) denotes the position of zero frequency. Reproduced from [33].

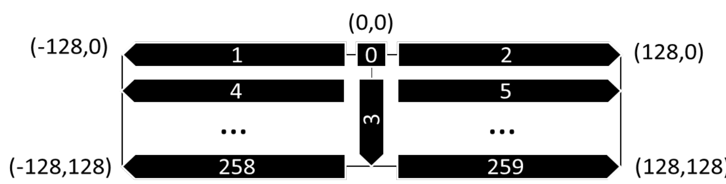

Figure 9. Scan order of Fourier coefficients in A. G. Tescher's algorithm [33].

Figures 8 and 9 illustrate additional details of A.G. Tescher's algorithm. Figure 8 shows the arrangement of the Fourier coefficients in the encoding algorithm. Only the lower (negative direction) rows of spectral images are encoded. The upper ones are discarded as redundant due to the conjugate symmetry. Figure 9 describes the scan pattern. It includes several "walks" from central (higher amplitude) positions to the boundary. For instance, segments 1 and 2 denote horizontal scans from the DC to higher frequencies. Segment 3 performs descent in the vertical direction. The remaining horizontal scans cover the rest of the surface.

While not as elegant as a continuous zigzag scan in the later algorithms, this pattern serves the same fundamental purpose. It enables efficient progressive coding of transform coefficients. Effectively, the scan order shown in Figure 9 is the predecessor of the zigzag scan!

2.4. Ad-hoc DCT Computation. Manhattan distance. Diagonal zones. Diagonal scans.

In 1973, Bernie (W.B.) Schaming of RCA Corporation developed his own Fourier transform-based image codec. The RCA research report RE-20-1-10, dated December 1973, offers the first description of this algorithm [35]. It subsequently appears in the June-July 1974 issue of the RCA Engineer journal [36].

This codec is interesting in two aspects.

The first is the all-real implementation of the Fourier transform. As shown in Figure 10, this algorithm takes a 4x4 subpicture from the input image and then turns it into an 8x8 subpicture by symmetrically folding it horizontally and vertically. Such symmetric expansion makes Fourier coefficients real and equal in all quadrants. Hence, only one quadrant needs to be encoded and transmitted.

b_{11}	b_{12}	b_{13}	b_{14}	b_{14}	b_{13}	b_{12}	b_{11}
b_{21}	b_{22}	b_{23}	b_{24}	b_{24}	b_{23}	b_{22}	b_{21}
b_{31}	b_{32}	b_{33}	b_{34}	b_{34}	b_{33}	b_{32}	b_{31}
b_{41}	b_{42}	b_{43}	b_{44}	b_{44}	b_{43}	b_{42}	b_{41}
b_{41}	b_{42}	b_{43}	b_{44}	b_{44}	b_{43}	b_{42}	b_{41}
b_{31}	b_{32}	b_{33}	b_{34}	b_{34}	b_{33}	b_{32}	b_{31}
b_{21}	b_{22}	b_{23}	b_{24}	b_{24}	b_{23}	b_{22}	b_{21}
b_{11}	b_{12}	b_{13}	b_{14}	b_{14}	b_{13}	b_{12}	b_{11}

Figure 10. Symmetric extension of 4x4 subpicture into 8x8 subpicture used as input to 2D Fourier transform. Reproduced from [35].

According to [35], this design was motivated by the desire to avoid the "extraneous high-frequency energy in the spectrum" caused by the block-based application of the transform. What W. B. Schaming did not realize, however, is that this construction has produced a different kind of transform. He was effectively computing the Discrete Cosine Transform of type II (DCT-II) [56,57]! This algorithm was likely the first image codec using the DCT! It was invented and designed before the term "Discrete Cosine Transform" was introduced to the public in N. Ahmed, T. Natarajan, and K.R. Rao's paper [56], appearing in January 1974 (see also [58,59]).

The second important technique introduced in W. B. Schaming's paper is zonal sampling by *diagonal bands*. He defines coefficient zones as "bands, positioned at equal Manhattan distance from the DC coefficient $C_{0,0}$. [The Manhattan distance is defined as the number of increments in the x and y direction from $C_{0,0}$ to $C_{i,j}$]." Figure 11 reproduces zonal arrangement and bit-assignments in W. B. Schaming's algorithm [35].

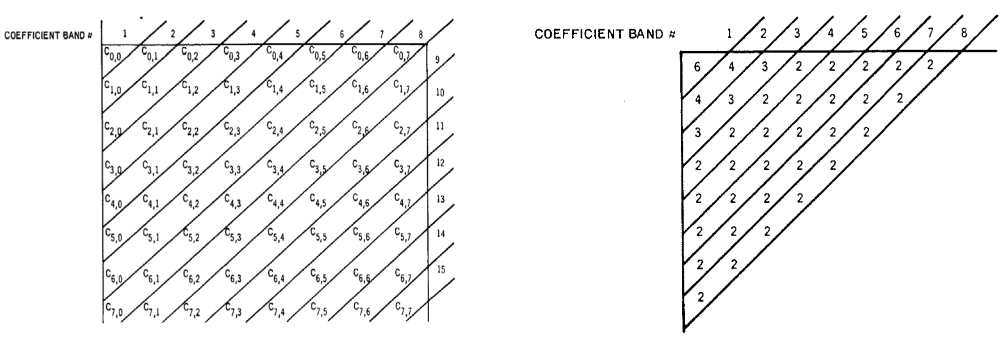

(a) Diagonal bands. (b) Bit-allocation to coefficients in each band.

Figure 11. Arrangement of zones ("diagonal bands") and bit-allocation implemented in W. B. Schaming's encoder. Reproduced from [35].

As a justification for this arrangement, W. B. Schaming notes: "The variance of any coefficient taken from the sub-pictures in the image tends to decrease with increasing band number since the energy content of most images decreases with increasing spatial frequency. This seems to be supported by the findings of Landau and Slepian [29]. Furthermore, our observation has been that all coefficients within a band of equal Manhattan distance tend to have comparable variances".

In other words, W. B. Schaming relied primarily on intuition and empirical evidence. However, to a considerable extent, this theory can also be supported by using the Lukosz bound argument. For instance, if we walk along diagonals over the 2D Lukosz surface (cf. Figure 7), we observe at most a factor of $\sqrt{2}$ gap in magnitudes. If magnitude ranges are similarly bounded, the variances should be similarly bounded as well (see Appendix A for extra mathematical details). This connection is not perfect, but it shows that this theory has a basis. The variance limits are lower for higher frequency bands. Notably, the diagonal bands model is simple. Simplicity wins in practical designs!

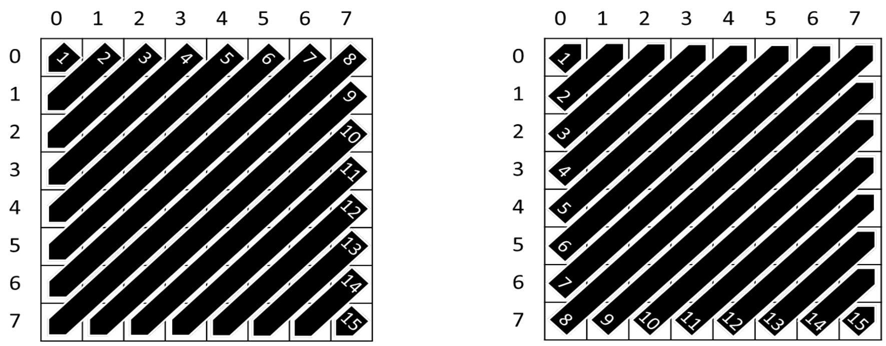

(a) Top-left scan. (b) Up-right scan.

Figure 12. Possible scan orders in W. B. Schaming's algorithm [35]. (a) top-left, (b) up-right diagonal scan orders.

From the description of W. B. Schaming's algorithm [35], it follows that to encode the transform coefficients, one needs to process them in zonal order, effectively moving from band 1 (DC) to band 15 (see Figure 11(a)), and then quantize and send coefficients within each band. This description allows at least two possible scan orders, depicted in Figure 12. The first (a) is a "top-left" diagonal scan pattern, and the second (b) is an "up-right" diagonal scan.

Looking at Figure 12, we observe patterns that look much closer to the zigzag scan!

2.6. The first appearance of the Zigzag scan

The first complete shape of the zigzag scan order appears in a 1975 paper authored by J. R. Parsons and A. G. Tescher and entitled "An Investigation of MSE Contributions in Transform Image Coding Schemes" [37].

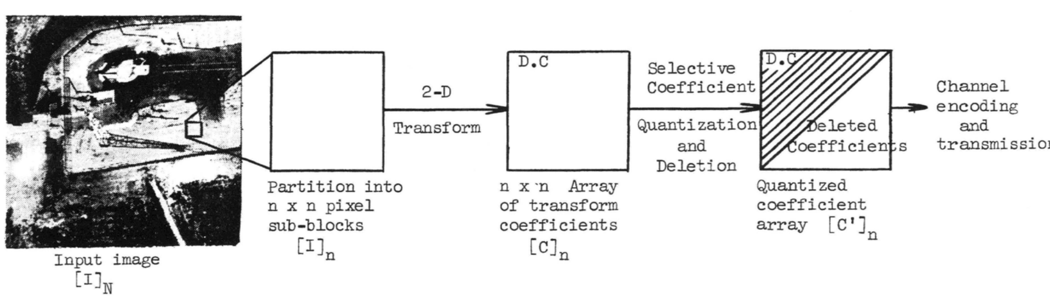

Figure 13. Overall processing model in the Parsons-Tescher encoders. Reproduced from [37]. © SPIE 1975.

As shown in Figure 13, the Parsons-Tescher encoder partitions an input image into $n \times n$ sub-blocks. Each sub-block is then transformed and encoded by applying quantizers for coefficients in each diagonal zone. Figure 14(a) shows the diagonal zones used for bit-allocation and quantizer design. Figure 14(b) shows "coefficient ordering" for encoding and transmitting the coefficients. This coefficient ordering is now exactly and precisely the zigzag scan!

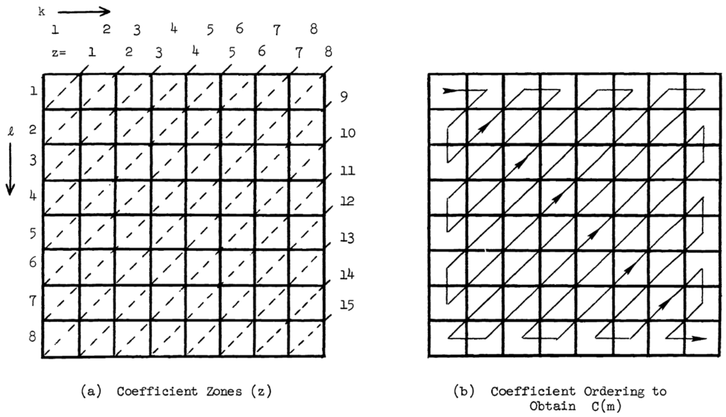

Figure 14. (a) Diagonal zones, and (b) Scan order implemented in the Parsons-Tescher encoder. Reproduced from [37]. © SPIE 1975.

We note that Parsons and Tescher's study [37] is not limited to a specific encoding scheme. Instead, it describes a framework in which they tested many codecs. They tried different transforms (Fourier, Cosine, Slant, and Hadamard), block sizes (8x8 and 16x16), quantizers (uniform, Gaussian, and adaptive quantization), and various bitrates and bit-allocation schemes. The zigzag scan worked universally to support all such implementations. Effectively, this paper not only brings the first description of the zigzag scan but also demonstrates the remarkable versatility of this technique.

2.7. Tescher-Cox's adaptive transform coding algorithm

We next review the 1976 paper of A.G. Tescher and R. V. Cox [38] (see also [39]), entitled "An adaptive transform coding algorithm." This paper combines the original ideas of adaptive coding of amplitude Fourier spectrum from [33,34] with an architecture employing the DCT transform and the zigzag scan pattern [37]. It is also the earliest reference that introduces the term "zigzag" scan.

Figure 15 reproduces a few pictures from the original paper [38], explaining the key concepts. As in the Parsons-Tescher's framework [37], the image is partitioned into 16x16 or 32x32 subblocks; each subblock is DCT-transformed, the DCT coefficients are scanned using a zigzag pattern, then quantized and encoded.

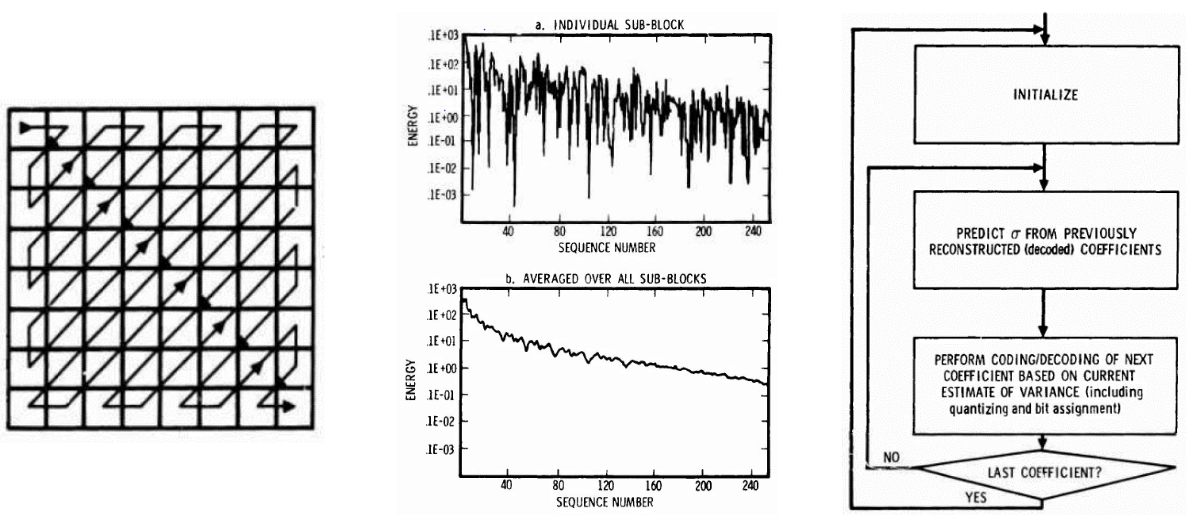

(a) Coefficient scan order. (b) Variances of coefficients. (c) Adaptive coding process.

Figure 15. Principles of operation of Tescher-Cox encoder [38]. (a) Scan order. (b) Variances of transform coefficients in the scan order. (c) Flow-graph of adaptive coding algorithm. Reproduced from [38]. © IEEE, 1976.

The quantization process is adaptive. It uses the coefficient's variance estimates to define the required bit allocation and set the reconstruction levels. For the first coefficient, the variance is sent as side information. For subsequent coefficients, the variance estimate is computed as a weighted average of variances of previously encoded and transmitted coefficients. Simple exponential weighting average logic is used. The subfigures in Figure 16(b) show the distributions of variances of 16x16 DCT coefficients along zigzag scan order as measured for a single sub-block and across all sub-blocks in an image. These distributions explain why variance-based prediction along the zigzag scan order is effective.

A.G. Tescher and R.V. Cox's paper [38] is likely the best-known reference on the origin of the zigzag scan. It is cited by several subsequent publications [7,11,42-47], including the classic books by K.R. Rao [7,11]. It presents the most compelling argument for this concept. However, as we have seen from our review, the original ideas that led to this technique began to appear much earlier [33-36].

Importantly, we have discovered that the idea of an optimal (and universally applicable to all images) scan order has emerged in the era of Fourier-based coding algorithms. This idea predates the introduction of the DCT [56] and the subsequent evolution of DCT-based image codecs. It is one of the earliest and most fundamental techniques in transform-based picture coding.

3. EVOLUTION OF CODEC ARCHITECTURES. NEW USES OF THE ZIGZAG SCAN.

3.1. The evolution of early codec architectures. Convergence toward DCT.

The late 1960s – early 1970s saw the rise of many alternative image compression algorithms [31,41,43]. In addition to the Fourier-based designs [16-18], there was a surge of interest in Walsh-Hadamard transforms [19-21,26-28], as well as Slant transform-based codecs [18,32]. The use of the Karhunen–Loève transform (KLT) has also started gaining traction due to the efforts of A. Habibi and P. Wintz [21-24], M. Tasto and P. Wintz [30], A.K. Jain [43], et al. Theoretically, KLT seemed the best, but it was very complex to compute. No fast algorithms existed.

The challenge posed by KLT implementations attracted the attention of Nasir Ahmed of the University of New Mexico. As he explains in [58], he started working on this problem in 1971. He looked at the KLT basis functions for the AR-1 process and tried to find a sinusoidal-family transform with similar responses. The criterion of effectiveness was the decay of variances of higher-order harmonics. The final result was the famous N. Ahmed, T. Natarajan, and K.R. Rao's paper [56], appearing in print in January 1974. In Figure 16, we reproduce the comparison of DCT vs KLT and other transforms, as reported in [56].

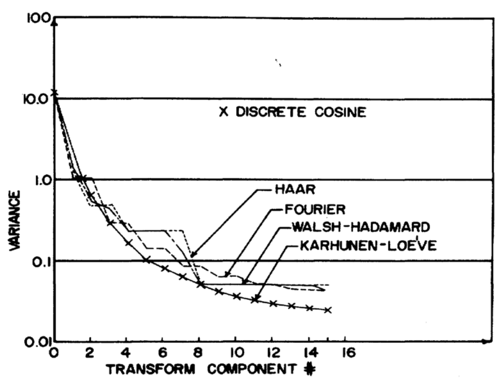

Figure 16. Comparison of efficiencies of different transforms as reported in the paper by N. Ahmed, T. Natarajan, and K.R. Rao [56]. The results are for transforms of size N=16 and AR-1 process with $\rho = 0.95$. © IEEE, 1974.

The arrival of the DCT was a turning point in image and video codec designs. DCT was faster and better than other transforms. In addition to the already mentioned designs by Parsons-Tescher [37] and Tescher-Cox [38], many others have followed. Starting from the late 1970s, most image and video codecs were DCT-based. However, most encoders of that era still employed rather complex quantization schemes, with Lloyd-Max-type quantizers, variable bit-allocation, and various zone-level or block-level adaptation or classification techniques [38-43].

3.2. Compression Labs. Chen-Pratt's Scene Adaptive Encoder.

The next significant development in the evolution of image and video codecs was an algorithm designed by Wen-Hsuing Chen and William K. Pratt of Compression Labs, Inc., San Jose, CA. The description of this algorithm first appeared in a conference paper [45] in 1981, followed by a journal paper [46] in 1984. The same algorithm was also the basis for the hardware video conferencing product introduced by Compression Labs in 1982 [60,61].

Chen-Pratt's encoder brings a fusion of ideas from several previous algorithms [25,30,37,38,40], along with significant simplifications in the design of the quantizers. The simplifications were necessary for reducing hardware costs. The ability to implement the encoder as a single-pass process was another critical design objective [45].

Figure 17 presents the overall block diagram of this algorithm.

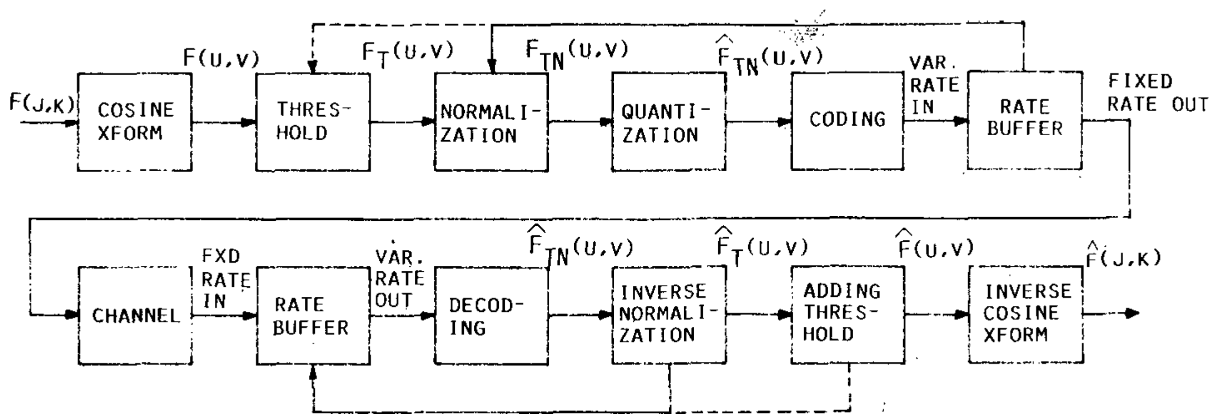

Figure 17. Principles of operation of W-H. Chen and W. K. Pratt's "Scene Adaptive Coder." Reproduced from [45] © IEEE, 1984.

As a core transform, Chen-Pratt's codec uses 16x16 DCT. The zigzag scan is also employed. Then follows a scalar uniform quantizer with dead-zone threshold logic. As illustrated in Figures 17 and 18, the quantization process includes two control parameters: 1) the dead-zone threshold parameter T and 2) the quantizer scale (normalization) factor D. If the coefficient's amplitude $|x|$ is less than T, it becomes 0, otherwise the nearest integer to $(|x| - T)/D$ is produced. Both parameters are adjusted on a subblock basis based on the feedback from the rate buffer. As the paper [45] explains, this rate control loop enables the encoder to work as a single-pass process.

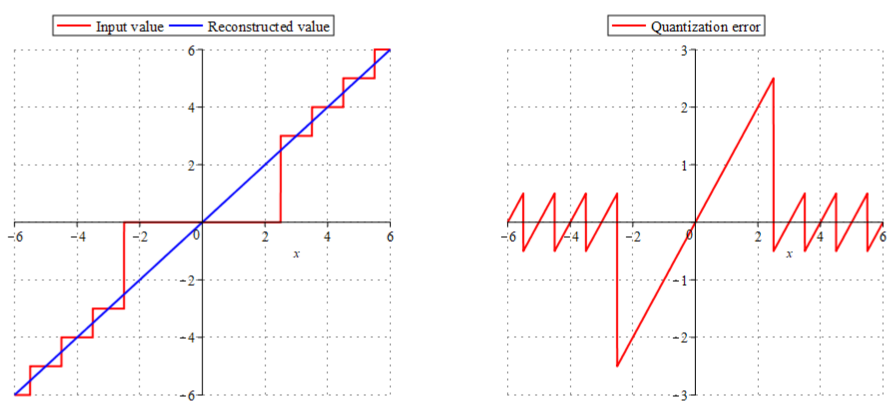

Figure 18. Quantizer design in Chen-Pratt codec [45]. Plots produced for threshold T=2 and normalization factor D=1. The effective dead zone in this quantizer is [-T -D/2, T + D/2]. With T=0, it turns into a classic mid-tread quantizer.

I. Codes for coefficients' amplitudes.

AMPLITUDE	NUMBER OF CODE BITS	HUFFMAN CODES
1	1	1
2	3	001
3	4	0111
4	5	00001
5	5	01101
6	6	011001
7	7	0000001
8	7	0110001
9	8	00000000
10	8	01100000
11	8	00000001
12	8	01100001
13	6+8	000001+8 BITS
EOB	4	0001
RL PREFIX	3	010

II. Codes for the numbers of consecutive zero-valued coefficients.

RUN-LENGTH	NUMBER OF CODE BITS	HUFFMAN CODE	RUN-LENGTH	NUMBER OF CODE BITS	HUFFMAN CODE
1	2	11	16	6	000011
2	3	101	17	6	001011
3	3	011	18	7	0000000
4	4	0101	19	7	0000100
5	4	0011	20	7	0000010
6	5	01000	21	7	0001110
7	5	10010	22	7	0000001
8	5	01001	23	7	0000101
9	5	10001	24	7	0000011
10	5	10011	25	7	0001111
11	6	001000	26	8	00011000
12	6	100000	27	8	00011010
13	6	001010	28	8	00011001
14	6	001001	29	8	00011011
15	6	100001	30	5+8	00010+8 BITS

Figure 19. Huffman codes for absolute values and zero-runs of transform coefficients in W-H. Chen and W. K. Pratt's "Scene Adaptive Coder." Reproduced from [45] © IEEE, 1984.

The algorithm also employs Huffman codes, as shown in Figure 19. One table is for amplitudes of the non-zero coefficients, and another is for lengths of zero sequences. The signs of non-zero coefficients are transmitted directly.

As we immediately notice, this design looks remarkably similar to intra-coding tools in H.261/3 and MPEG-1/2 codecs, appearing in the early 1990s. This algorithm has offered a blueprint for the design of these early standards.

3.3. New uses of the zigzag scan.

Recall that in the earlier designs [37-40], the purpose of the zigzag scan was to ensure progressive decay of variances of coefficients. It was essential for the predictive design of quantizers. However, the Chen-Pratt algorithm [45] has thrown away predictive quantization logic. It changed the utility of the zigzag.

Intuitively, the utility of the zigzag scan in the Chen-Pratt design [45] boils down to *maximizing the lengths of runs of zero-valued coefficients*. The longer the runs, the fewer Huffman codewords are sent to the decoder, leading to a more compact code overall. The reason the zigzag scan helps is its variance-sorting property. It pushes all low-variance coefficients to the end. If a coefficient in some position falls below the threshold, it increases the chances that the subsequent coefficients will also turn to zero.

However, this is only one plausible explanation of the function of the zigzag scan.

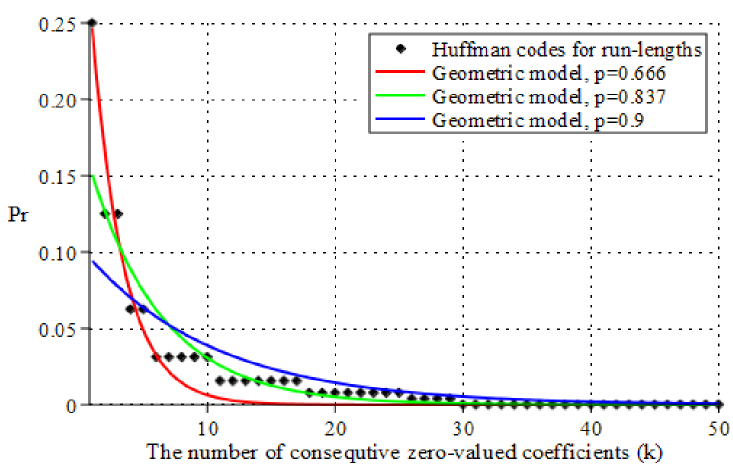

Figure 20. Probabilities of run-lengths implied by Huffman codes [45] vs. geometric model: $\Pr(k) = (1-p) \cdot p^{k-1}$. Probabilities of longer runs (k) are better matched by models with larger values of model parameter p.

To gain additional insights, in Figure 20, we analyze the shape of the run-length distribution implied by Huffman codes in Chen-Pratt's encoder [45]. The implied probabilities of runs k are computed as $\Pr(k) = 2^{-\text{CodeLength}(k)}$. The reference geometric model used for analysis: $\Pr(k) = (1-p) \cdot p^{k-1}$, where p is the model parameter. This model works if zeros are produced by independent and identically distributed (IID) variables. However, as Figure 20 shows, this model offers reasonable fits only for the limited range of run values k. For example, for small runs (k=1...4), a good fit is achieved by a model with p=0.666. For mid-range runs (k=8...20), the model with p=0.837 works better. For long runs (k=40+), the model with p=0.9 is the better approximation.

What does this observation mean? It means that this Huffman table was constructed for *compound distribution*. At higher values of zero runs (k), we see contributions of coefficients with higher zero probability (lower variance). At lower runs, we capture coefficients with lower zero probability (higher variance). Effectively, this Huffman table captures the *decay of variances* of transform coefficients along the zigzag path! This observation brings a more direct connection between Chen-Pratt's design and the original intent and purpose of the zigzag scan.

Importantly, we now also see a more general utility of the zigzag scan in lossless coding. Grouping coefficients with similar variances together *minimizes the divergence of their distributions,* enabling more effective joint (block) or predictive coding. It is the fundamental reason it helps in any lossless coding scheme.

In their paper [45], Chen and Pratt mention one extra optimization method related to the zigzag scan: "There are many ways to improve the coding efficiency of the coder. One way is to cut down the number of runs in the run length coder. This can be accomplished by skipping single isolated coefficients with absolute magnitude of one". This optimization method is indeed essential and had many reappearances in subsequent encoder designs [62,63]. In passing, we must also mention that the dead zone thresholding logic in uniform quantizer design can be more sophisticated. References [64-66] pose the related optimization problem and offer methods adopted in more recent algorithms.

4. SCAN ORDERS IN IMAGE AND VIDEO COMPRESSION STANDARDS

4.1. CCITT T.120 Part 3. First DCT-based Video Codec proposal (1984)

The first (or at least the earliest known to the author) submission of a DCT-based algorithm for standardization occurred in November 1984 [67,68]. It was document number 4, submitted to the first meeting of the CCITT Specialists Group on Coding for Visual Telephony (CCITT Study Group XV, Working Party XV/1, Question 4), December 1984, Tokyo, Japan.

Annex A in this document [68] was authored by Compression Labs Inc. It describes an algorithm architecturally similar to the Chen-Pratt encoder [45], with an added DPCM coding module after the transform. The contribution explains that this DPCM module performs temporal and spatial prediction. The proposal precisely defines the DCT transform and the zigzag scan order. We reproduce a few images from this document in Figure 21.

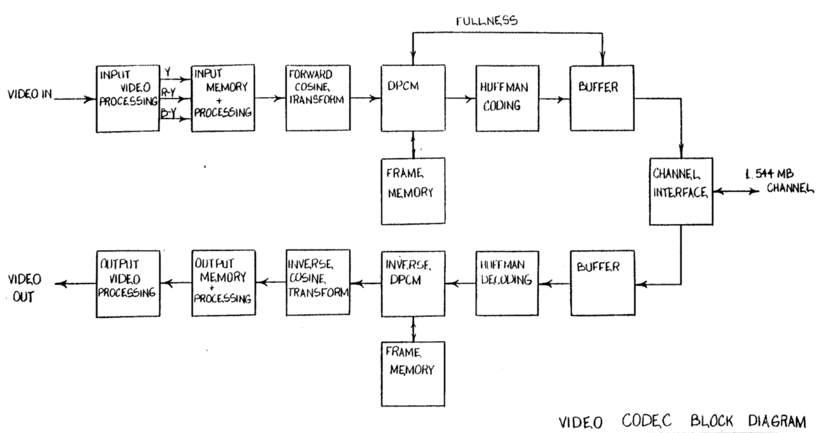

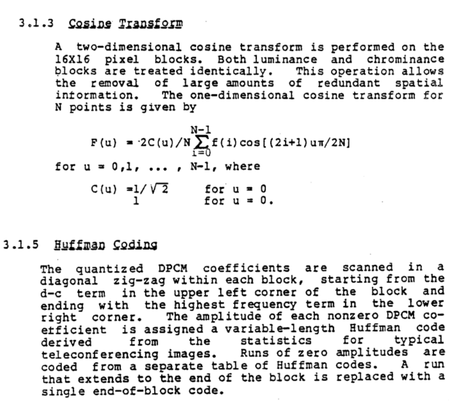

3.1.3 Cosine Transform

A two-dimensional cosine transform is performed on the 16X16 pixel blocks. Both luminance and chrominance blocks are treated identically. This operation allows the removal of large amounts of redundant spatial information. The one-dimensional cosine transform for N points is given by

$$F(u) = 2C(u)/N \sum_{i=0}^{N-1} f(i) \cos[(2i+1)u\pi/2N]$$

for u = 0,1, ... , N-1, where

$$C(u) = \begin{cases} 1/\sqrt{2} & \text{for } u = 0 \\ 1 & \text{for } u = 0. \end{cases}$$

3.1.5 Huffman Coding

The quantized DPCM coefficients are scanned in a diagonal zig-zag within each block, starting from the d-c term in the upper left corner of the block and ending with the highest frequency term in the lower right corner. The amplitude of each nonzero DPCM coefficient is assigned a variable-length Huffman code derived from the statistics for typical teleconferencing images. Runs of zero amplitudes are coded from a separate table of Huffman codes. A run that extends to the end of the block is replaced with a single end-of-block code.

Figure 21. Images from Compression Labs video codec proposal submitted for standardization in 1984 [68].

This proposal was initially submitted for inclusion in Part 3 of the second version of the CCITT Recommendation H.120 [69]. The CCITT (International Telephone and Telegraph Consultative Committee) would later become the ITU-T (the International Telecommunication Union – Telecommunication Standardization Sector) in 1992.

4.2. CCITT H.261 (1985-1990). ITU-T H.263 (1992-1996)

According to G. J. Sullivan [67], while Part 3 of H.120 did not ultimately use a DCT-based design when it was finalized in 1988, such a design would soon become the prime candidate for the next international video coding standard [7,70], which would become the Recommendation H.261 [2] in 1990. The third meeting of the CCITT SGXV Specialists Group in September 1985 would bring two more substantial DCT-based proposals [71,72], and the fourth and fifth would bring more. By the fifth meeting in March 1986, the team had converged on a DCT-based design [73] using an 8×8 block size with 4:2:0 sampling such that the area of one 8×8 chrominance (chroma) block corresponded with four 8×8 luminance (luma) blocks. This was coupled with block-wise motion compensation, zigzag scanning, scalar quantization with a uniform step size (and an expanded dead zone), variable-length coding, picture start codes, a "group of blocks" with an associated start code, and other design components to form what we can recognize today as the heart of H.261 and several designs that followed it.

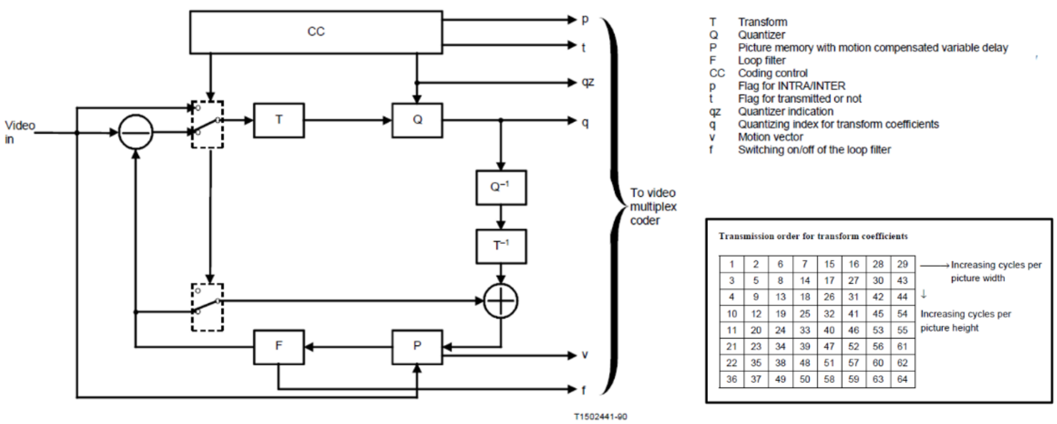

Figure 22. The overall block diagram and scan order adopted in the H.261 standard [2].

The first text of the H.261 standard was ratified in November 1988. The complete specification [2] was published in December 1990. The same 8x8 DCT transform and zigzag scanning process also appear in the ITU-T Recommendation H.263 [74], developed as a sequel to the H.261 recommendation in 1992-1996. We show the overall architecture of the H.261 codec and its definition of the scan pattern in Figure 22.

4.3. CCIR CMTT 723 (1985-1993)

The CCIR CMTT 723 was another early video coding standard developed in the CMMT (the Committee for Mixed Telephone and Television), a joint activity between the CCIR (International Radio Consultative Committee) and the CCITT. The Interim Working Party (IWP) CMTT/2, formed in 1985, was tasked with developing this codec [75].

According to A. N. Heightman [76], the first DCT-based proposals to this standard appeared in May 1987. The selection and evaluation process was concluded in June 1989. The first draft specification was published in June 1990 in the CCIR Plenary Report [75]. Subsequently, this algorithm was refined in 1990-1992 by a joint activity between EBU and ETSI (European Telecommunications Standards Institute) [77,78]. The result was a European standard ETS 300 174, published in November 1992 [79]. The international version was published as ITU-T Recommendation J.81 in September 1993 [80].

The interim CMTT 723 specification [75] presented all essential elements of a hybrid DCT-based video codec. It differed from CCITT Rec. H.261 in several aspects. It used half-pixel motion compensation. It applied different quantization with no dead zone but added "relative visibility matrices" to shape noise towards higher frequencies. Moreover, it also used different scan orders for luma and chroma components.

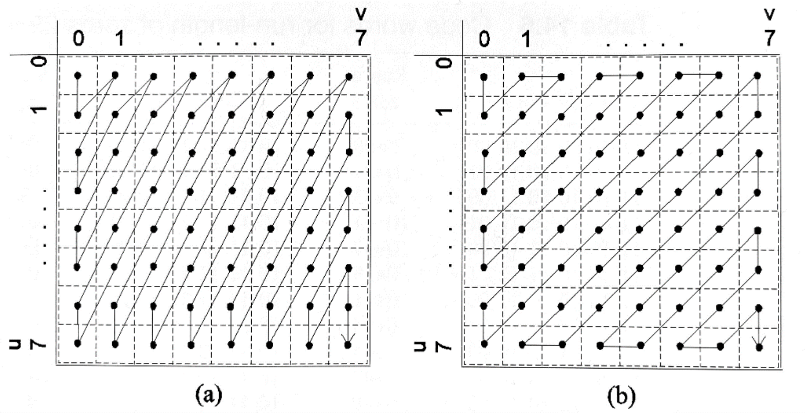

Figure 23. Coefficient scan orders as defined in CCIR CMTT 723 (ITU-T J.81) standard [79].
(a) Luminance scan. (b) Chrominance scan.

The main reason for introducing two different scan patterns was the 4:2:2-sampled interlaced video format. Vertical correlation in the luma plane was weaker. The solution was a luma scan with twice faster descent vertically than horizontally. The chroma coding used a more traditional zigzag scan in the "up-right" direction. We reproduce the scan orders adopted in CMTT 723 / ITU-T J.81 standard in Figure 23.

4.4. JPEG (1986-1992). MPEG-1 (1988-1991)

The history of both JPEG and MPEG-1 standards is well known [8-11,81-90]. The DCT-based architecture of JPEG came from the ADCT (Adaptive DCT) algorithm proposal [82,83], developed as part of the European collaborative project PICA [83] under the ESPRIT [84,85] program. It was submitted to JPEG for evaluation in June 1987 [86].

Architecturally, the ADCT algorithm was similar to Parsons-Tescher codecs [37]. It used DCT and zigzag scan. The unique addition (and hence the name "adaptive") was hierarchical coding and transmission mode [82]. The quantizer design was also substantially different, employing a noise-shaping matrix selected based on psychophysical studies [86,88].

The 1988 paper by A. Leger, J. L. Mitchell, and Y. Yamazaki [88] describes the selection process used by JPEG. It mentions that one of the advantages of choosing ADCT as a basis for the standard was tool-level compatibility with DCT-based video codecs under development in CCITT SGXV and CCIR. In other words, JPEG experts were aware of efforts towards H.261 and CMTT 723, and the eventual commonality between these codecs was the intended effect.

The MPEG-1 standard [91], developed in 1988-1990 after the JPEG algorithm was already defined, had a similar design philosophy. The compatibility with JPEG for intra-coding tools was desirable to ease hardware implementations [9,89]. The eventual specification of the 8x8 DCT and the zigzag scan in MPEG-1 standard [91] is identical to the ones defined in JPEG and H.261 standards [1,2].

4.5. MPEG-2 (1992-1994)

The MPEG-2 video standard has extended the MPEG-1 specification. Importantly, it added support for interlace video coding. It was submitted for publication as ISO/IEC 13818-2 in October 1994 [92]. ITU-T also published this standard as ITU-T Recommendation H.222 in October 1995 [93].

As shown in Figure 24, MPEG-2 has added an "alternative scan" for interlaced content in addition to the traditional zigzag scan order. Similarly to the design of the luma scan order in CMTT 723, the alternative scan order in MPEG-2 uses faster descent in the vertical direction. However, the shape of this scan order is somewhat different.

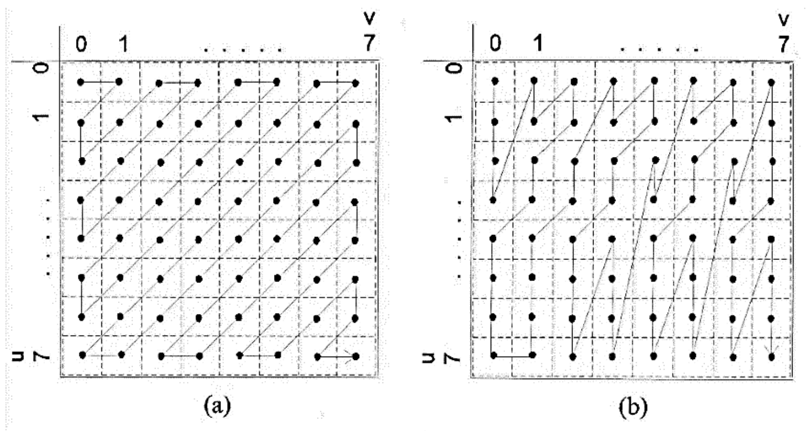

Figure 24. Coefficient scan orders as defined in MPEG-2 standard [92,93]. (a) Zigzag scan. (b) Alternative scan.

4.6 ITU-T H.264 | MPEG-4 AVC standard (1998-2005)

The ITU-T Rec. H.264 | MPEG-4 AVC (Advanced Video Coding) standard [94,95] was developed in the late 1990s – early 2000s. It uses integer approximations of 4x4 and 8x8 DCT transforms coupled with two types of zigzag scan patterns. The use of integer transforms was suggested by G. Bjontegaard in December 1997 [96].

Figure 25 shows scan orders adopted in H.264: the regular zigzag and the "field scan" for coding interlaced sources. The objective of the field scans in H.264 is the same as in CMTT 723 and MPEG-2 codecs, but the final shapes are somewhat different.

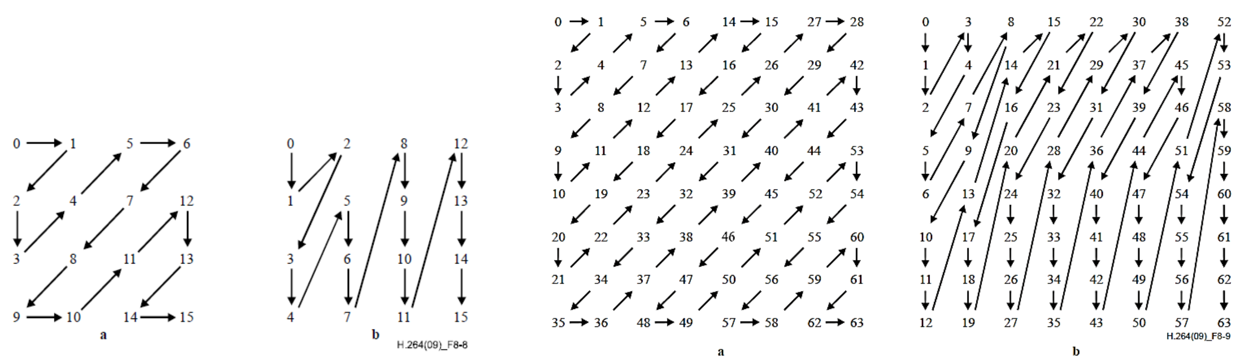

Scan orders for 4x4 blocks

Scan orders for 8x8 blocks.

Figure 25. Scan orders adopted in the H.264/AVC standard [94,95] (a) Zigzag scans. (b) Field scans.

4.7 JPEG-XR standard (2007-2010)

JPEG-XR (JPEG Extended Range) standard [97,98] was developed in the 2006-2010 timeframe. It has brought several innovations, including integer-reversible hierarchical lapped transforms [99,100] and dynamic adaptations of scan orders [101].

The two possible initial scan orders, as defined by the JPEG-XR standard, are illustrated in Figure 26. Only AC coefficients are enumerated. The scan order in Figure 26(a) is consistent with the design of a classic zigzag scan. The alternative scan order in Figure 26(b) is somewhat different. It uses a faster descent horizontally than vertically (which likely helps with anamorphic images). The adaptation process is performed for each tile within an image, starting with an initial scan pattern and then allowing occasional incremental swaps of scan points (similar to a bubble sort process) if the statistics of encountered zero coefficients indicate that it will be more efficient [101].

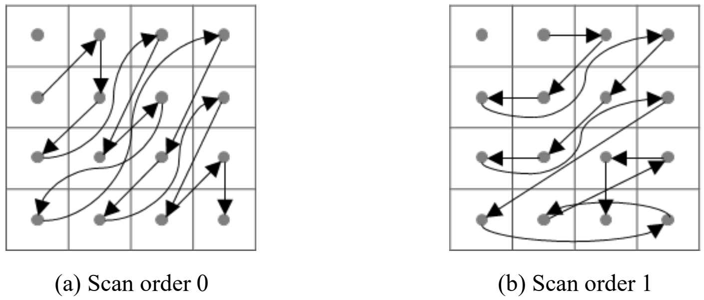

Figure 26. Initial scan orders used in JPEG-XR standard [97,98].

4.8 ITU-T H.265 | MPEG-H HEVC standard (2010-2015)

The ITU-T Rec. H.265 | MPEG-H HEVC (High-Efficiency Video Coding) standard [102,103] was developed in the 2010-2015 timeframe. It allows several transform sizes, from 4x4 to 32x32, and two kinds of transforms: the classic DCT-II [56] and DST-VII [104-106], which became helpful for coding intra-predicted content [107,108]. It also uses several scan orders, as shown in Figure 27. The "up-right diagonal" scan (Figure 27(a)) is a variant of the classic zigzag scan. Additional horizontal and vertical scans are allowed for Intra-coding.

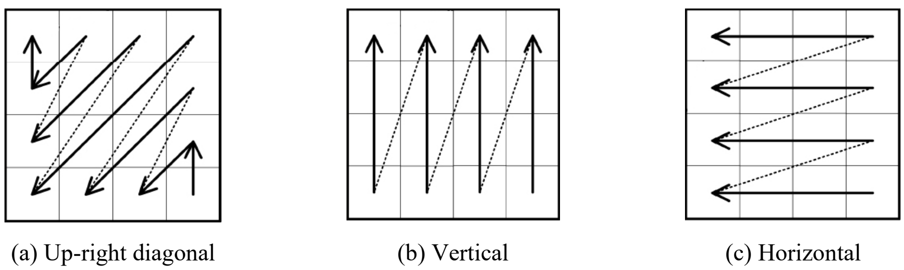

Figure 27. Illustration of scan orders adopted in the HEVC standard [94,95].

When working with block sizes larger than 4x4, the HEVC standard employs a secondary diagonal scan order. We illustrate this in Figure 28. An 8x8 block becomes partitioned into four 4x4 sub-blocks. The coefficients within each block are enumerated using the diagonal scan order. Then, the secondary diagonal scan enumerates the subblocks. As explained in [109], the rationale for this design was convenience for modular and parallel processing implementations.

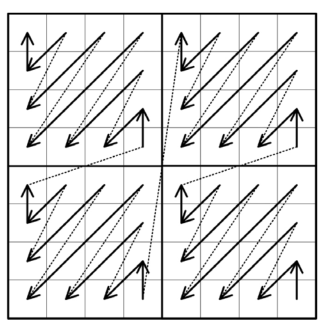

Figure 28. A two-level diagonal scan pattern for 8x8 block in HEVC standard [94,95].

4.9 ITU-T H.266 | MPEG-I VVC standard (2016-2020)

Finally, we look at the VVC (Versatile Video Coding) standard [110,111], developed in the 2016-2020 timeframe. This standard uses a broader set of transform sizes and types, including integer approximations of DCT-II, DST-VII, and DCT-VIII transforms. As the second stage transforms, VVC employs the so-called Low-Frequency Non-Separable Transforms

(LFNST) [112]. It also adds many other advanced technologies (loop filters, decoder-side refinement of motion vectors, more advanced quantization, etc). But it still uses the "up-right diagonal" scan – a close variant of the classic zigzag scan!

Overall, we can see from this survey that the zigzag scan introduced in the early 1970s still exists, driving the encoding of spectra produced by various transforms, predictors, and quantizers in modern generation image and video coding algorithms. It is one of the most original and fundamental techniques in this field!

5. CONCLUSIONS

We have studied the history of the development and modern uses of the zigzag scan in image and video coding algorithms. Our contributions are primarily in historical and methodological domains.

We have shown that the first scan orders were developed in the early 1970s, in the era of Fourier-transform-based codecs. The original reasoning for the 2D scan order was motivated by the Lucosz bound. It states that the amplitude range of Fourier spectra progressively decays with higher frequencies. This bound holds for all non-negative signals, suggesting that a single scan order can work universally for all images. In application to statistical models, the Lucosz bound translates to bounds on variances. This theory connects well with the "diagonal zoning" concept and the "zigzag" shape of the scan pattern introduced subsequently. The first papers in which the zigzag scan pattern emerged were Parsons and Tescher [37], 1975, and Tescher and Cox [38], 1976.

We also traced the evolution of codec architectures, involving changes in the choices of transforms and designs of quantizers and the resulting changes in functions of the zigzag scan. The original intent of the zigzag scan in the Tescher-Cox coder [38] was to drive adaptive quantization of transform coefficients. With the switch to uniform + dead zone quantizers in the Chen-Pratt [45] and subsequent codecs, the utility of the zigzag scan also changed. It becomes a tool for the optimization of lossless encoding. It is the primary function it serves in most algorithms today.

Finally, we trace the history of introducing DCT + zigzag-based algorithms in image and video coding standards. We show that the earliest such proposal came in 1984 from Compression Labs. We subsequently review the variants of scan orders adopted in H.261/3, CMTT 723, JPEG, MPEG-1/2, H.264/AVC, JPEG-XR, HEVC, and VVC codecs. We show that despite many changes in the transforms, predictors, filter, and entropy coding techniques proposed over the last five decades, the zigzag scan is still essential and employed in the design of all these algorithms.

ACKNOWLEDGMENTS

The author thanks Dr. Andrew G. Tescher for a discussion at the SPIE conference around 2012, pointing to the existence of the Lukosz bound and the associated theory that motivated the early development of the zigzag scan. This insight has sparked the author's interest in this topic.

The author also thanks Prof. Bernd Girod, Dr. Henrique Malvar, Dr. Gary J. Sullivan, and Dr. Joel Sole for reviewing the preliminary version of this paper and offering their comments. Their comments have helped to correct some inaccuracies, add extra material, and improve the presentation overall.

REFERENCES

[1] CCITT Rec. T.81, "Information technology—Digital compression and coding of continuous-tone still images—Requirements and guidelines," CCITT (now ITU-T) (September 1992).
[2] CCITT Rec. H.261, "Video codec for audiovisual services at p x 64 kbps /s," CCITT (now ITU-T) (December 1990)
[3] N. Ahmed and K.R. Rao, "Orthogonal Transforms for Digital Signal Processing (1 ed.)," Berlin Heidelberg New York: Springer-Verlag. (July 1975)
[4] W. Pratt, "Digital Image Processing," John Wiley & Sons, New York (1978).

[5] T. Lynch, "Data Compression Techniques and Applications," Lifetime Learning Pub. (1985).
[6] A. K. Jain, "Fundamentals of digital image processing," Prentice-Hall, Inc. (1989).
[7] K. R. Rao and P. Yip. "Discrete Cosine Transforms. Algorithms, Advantages, Applications," Academic Press (1990).
[8] W. Pennebaker and J. Mitchell, "JPEG Still Image Data Compression Standard," Springer (1993).
[9] J. Mitchell, W. Pennebaker, C. Fogg, and D. J. LeGall, "MPEG Video Compression Standard," Chapman & Hall, New York (1996).
[10] A. Netravali, and B. Haskell, "Digital pictures: representation, compression, and standards," Plenum Publishing, New York (1995).
[11] K.R. Rao and J.J. Hwang, "Techniques and standards for image, video, and audio coding," Prentice-Hall, Inc. (1996).
[12] W. F. Schreiber, "Picture coding," in Proceedings of the IEEE, 55 (3), 320-330 (March 1967).
[13] W. Pratt, "A bibliography on television bandwidth reduction studies," in IEEE Transactions on Information Theory, 13(1), 114-115 (January 1967).
[14] H. C. Andrews and W.K. Pratt "Fourier Transform Coding of Images," Hawaii International Conference on System Sciences, 677-679 (January 1968).
[15] H. C. Andrews and W. K. Pratt, "Television Bandwidth Reduction by Fourier Image Coding," Society of Motion Picture and Television Engineers, 103rd Technical Conference (May 1968).
[16] H. C. Andrews and W. K. Pratt, "Television Bandwidth Reduction by Encoding Spatial Frequencies," Journal Society of Motion Picture and Television Engineers, 77, 279-1281 (December 1968).
[17] W. K. Pratt, J. Kane, and H. C. Andrews, "Hadamard transform image coding," Proc. IEEE 57, (1969).
[18] W. K. Pratt and H. C. Andrews, "Transform image coding. Final report. No. USCEE-387." (1970). Online: https://ntrs.nasa.gov/api/citations/19700019694/downloads/19700019694.pdf
[19] J. W. Woods, "Video Bandwidth Compression by Linear Transformation," MIT QPR 91, 219-224 (October 1968).
[20] T. S. Huang and J. W. Woods, "Picture Bandwidth Compression by Block Quantization," Intern. Symp. of Information Theory, Ellenville, New York. (1969)
[21] A. Habibi and P. A. Wintz, "Optimum linear transformations for encoding two-dimensional data," School of Elec. Eng., Purdue Univ., Lafayette, Ind., Tech. Rep. TR-EE69-15 (May 1969).
[22] A. Habibi, "Linear transformations for encoding 2-dimensional sources," Ph.D. Thesis, Purdue Univ., Lafayette, IN (March 1970).
[23] A. Habibi and P. A. Wintz, "Linear transformations for encoding two-dimensional sources," Purdue Univ., Lafayette, IN, TR-EE 70-2 (1970).
[24] A. Habibi and P. Wintz, "Image Coding by Linear Transformation and Block Quantization," in IEEE Transactions on Communication Technology, 19 (1), 50-62 (February 1971)
[25] G. Anderson and T. Huang, "Piecewise Fourier Transformation for Picture Bandwidth Compression," in IEEE Transactions on Communication Technology, 19(2), 133-140 (April 1971).
[26] H. Enomoto and K. Shibata, "Features of Hadamard Transformed Television Signal," 1965 National Conference of the IECE of Japan, 881 (1965).
[27] H. Enomoto and K. Shibata, "Television Signal Coding Method by Orthogonal Transformations," 1966 Joint Convention of the IECE of Japan, 1430 (1966).
[28] H. Enomoto and K. Shibata, "Orthogonal Transform Coding System for Television Signals," in IEEE Transactions on Electromagnetic Compatibility, 13(3), 11-17 (Aug. 1971).
[29] H. J. Landau, and D. Slepian, "Some Computer Experiments in Picture Processing for Bandwidth Reduction," Bell System Tech. Jour., 1525-1540 (May-June 1971).
[30] M. Tasto and P. Wintz, "Image Coding by Adaptive Block Quantization," in IEEE Transactions on Communication Technology, 19(6), 957-972 (December 1971).
[31] P. A. Wintz, "Transform Picture Coding," Proc. IEEE 60 (7), 809-820 (July 1, 1972).
[32] W.K. Pratt, W-H., Chen, L. Welch, "Slant transform image coding," IEEE Transactions on Communications, 22(8), 1075-93 (August 1974).
[33] A. G. Tescher, "The role of phase in adaptive image coding." PhD dissertation, USC (1973).
[34] A. G. Tescher, "The role of phase in adaptive image coding," USC Image Processing Institute Report 510 (December 1973). Online: https://apps.dtic.mil/sti/pdfs/AD0777993.pdf
[35] W. B. Schaming, "Digital Image Transform Encoding," RCA Corporate Engineering Services, Report RE-20-1-10, (December 1973).

[36] W. B. Schaming, "Digital Image Transform Encoding," RCA Engineer, 20(1), 32-37 (Jun-Jul, 1974).
[37] J. R. Parsons and A. G. Tescher, "An Investigation of MSE Contributions in Transform Image Coding Schemes," Proceedings of SPIE, 196-206 (August 1975).
[38] A.G. Tescher, and R. V. Cox. "An adaptive transform coding algorithm." Proc. IEEE XII ICC 20-25 (1976).
[39] A.G. Tescher, and R. V. Cox. "An adaptive transform coding algorithm." Interim Report SAMSO-TR-76-183, The Aerospace Corporation. (April 1976) Online: https://apps.dtic.mil/sti/pdfs/ADA028840.pdf
[40] W-H. Chen and C. Smith, "Adaptive Coding of Monochrome and Color Images," in IEEE Transactions on Communications, 25 (11), 1285-1292 (November 1977).
[41] A. Habibi, "Survey of Adaptive Image Coding Techniques," in IEEE Transactions on Communications, 25(11), 1275-1284 (November 1977).
[42] A.G. Tescher, "Transform Image Coding," Report SAMSO-TR-78-127, The Aerospace Corporation (May 1978) https://apps.dtic.mil/sti/pdfs/ADA061656.pdf
[43] A.K. Jain, "Image data compression: A review." Proceedings of the IEEE, 69 (3), 349-389 (1981).
[44] W.-H. Chen and W. K. Pratt, "Scene Adaptive Coder," Proceedings of International Conference on Communications, Philadelphia, PA, 22.5.1-22.5.6 (June 1981).
[45] W.-H. Chen and W. Pratt, "Scene Adaptive Coder," IEEE Transactions on Communications, 32 (3), 225-232 (March 1984).
[46] T. Saito, H. Takeo, K. Aizawa, H. Harashima, and H. Miyakawa, "Adaptive discrete cosine transform image coding using gain/Shape vector quantizers," ICASSP '86. IEEE International Conference on Acoustics, Speech, and Signal Processing, Tokyo, Japan, 129-132 (1986).
[47] W. A. Pearlman, "Adaptive cosine transform image coding with constant block distortion," in IEEE Transactions on Communications, 38(5), 698-703 (May 1990).
[48] J. W. Cooley and J. W. Tukey, "An algorithm for the machine calculation of complex Fourier series," Math. Of Computing, 19, 297- 301 (April 1965).
[49] J.W. Cooley, P.A.W. Lewis, and P.D. Welch "Historical Notes on the Fast Fourier Transform," Proceedings IEEE, 55, 1675-1677 (October 1967).
[50] H. C. Andrews, "A high-speed algorithm for the computer generation of Fourier transforms," IEEE Trans. Computers (Short Notes), C-17, 37-75 (April 1968).
[51] H. C. Andrews, A. G. Tescher and R. P. Kruger, "Image processing by digital computer," in IEEE Spectrum, 9 (7), 20-32 (July 1972).
[52] W. Lukosz, "Übertragung Nicht-Negativer Signale durch Lineare Filter," Optica Octa, 9, 335-364 (1962).
[53] R. P. Boas & M. Kac, "Inequalities for Fourier transforms of positive functions," Duke Math. J. 12, 189-206 (1945).
[54] H. Zemanian, "Some inequalities for Fourier transforms," Proceedings of the American Mathematical Society, 8 (3), 468-475 (1957).
[55] J. E. M. Janssen, "Frequency-domain bounds for non-negative, unsharply band-limited functions," Journal of Fourier Analysis and Applications, 1 (1), 39-65 (1994).
[56] N. Ahmed, T. Natarajan, K.R. Rao," Discrete Cosine Transform" IEEE Trans. Computers, 90-93 (January 1974).
[57] R. M. Haralick, "A Storage Efficient Way to Implement the Discrete Cosine Transform," in IEEE Transactions on Computers, vol. C-25, no. 7, pp. 764-765, July 1976.
[58] N. Ahmed, "How I came up with the Discrete Cosine Transform," Digital Signal Processing, 1(1), 4-5 (1991).
[59] R.S. Stanković, and J. T. Astola. "Reminiscences of the Early Work in DCT: Interview with KR Rao," Reprints from the Early Days of Information Sciences. Tampere International Center for Signal Processing. (2012). Online: https://ethw.org/w/images/1/19/Report-60.pdf
[60] R. Srinivasan and K. R. Rao "Teleconferencing," Proc. SPIE 0528, Digital Image Processing, (July 1985).
[61] D. Bodson, Study of potential standardization of video teleconferencing systems. Volume 1 – Final report," NCS Technical Information Bulletin 83-4 (May 1983) Online: https://apps.dtic.mil/sti/pdfs/ADA132080.pdf
[62] G. Bjontegaard, "H.26L Test Model Long Term Number 7 (TML-7) draft0. – Section 4.5 Elimination of single coefficients in inter macroblocks," Document VCEG-M81, ITU-T SG16 VCEG, Austin, Texas, USA (April 2001).
[63] M. Karczewicz, P. Chen, Y. Ye, and R. Joshi "R-D based quantization in H.264", Proc. SPIE 7443, Applications of Digital Image Processing XXXII, 744314 (September 2009).
[64] G. J. Sullivan, "Efficient scalar quantization of exponential and Laplacian random variables," in IEEE Transactions on Information Theory, 42(5), 1365-1374 (September 1996)
[65] G. J. Sullivan, "Adaptive quantization encoding technique using an equal expected-value rule," Document: JVT-N011, Joint Video Team (JVT) of ISO/IEC MPEG & ITU-T VCEG, Hong Kong, China (January 2005).

[66] G. J. Sullivan, and S. Sun, "On dead-zone plus uniform threshold scalar quantization," Proc. SPIE 5960, Visual Communications and Image Processing 2005, 596033 (June 2005)
[67] G. J. Sullivan, "Standardization of IDCT approximation behavior for video compression: the history and the new MPEG-C parts 1 and 2 standards," Proc. SPIE 6696, Applications of Digital Image Processing XXX, 669611 (August 2007).
[68] United States of America, "Description of Two of the Video Codecs used in the United States with Primary Rate Transmission Systems," CCITT SG XV Specialists Group on Coding for Visual Telephony, Document #4 Annex A (Compression Labs section) (Nov. 1984).
[69] ITU-T Rec. H.120, Codecs for Videoconferencing using Primary Digital Group Transmission (ver. 1, 1984), (ver. 2, 1988).
[70] M. Liou, "Overview of the p × 64 kbit/s Video Coding Standard", Communications of the ACM, 34(4), 59-63 (April 1991).
[71] Sweden, Netherlands, France, Federal Republic of Germany, British Telecom (UK), and CSELT (Italy), "Hybrid Coding," CCITT SG XV Specialists Group on Coding for Visual Telephony document #36 (Sept. 1985).
[72] NTT, KDD, NEC, and Fujitsu, "Candidates for Subrate Coding Algorithm," CCITT SG XV Specialists Group on Coding for Visual Telephony document #43 (Sept. 1985).
[73] Chairman (S. Okubo), "Report of the Fifth Meeting in Tokyo," CCITT SG XV Specialists Group on Coding for Visual Telephony document #103R (March 1986).
[74] ITU-T Recommendation H.263, "Video coding for low bit rate communication," ITU-T (March 1996)
[75] CCIR, "Recommendations of the CCIR, 1990, Volume XII, Television and Sound Transmission (CMTT)", CCIR, XVII-th Plenary Assembly, Dusseldorf (May-June 1990).
[76] A. N. Heightman, "The work of CCIR Interim Working Parties 11/7 and CMTT/2 (on digital TV standards)." In IEE Colloquium on Emerging CCIR Standards for Digital Television Transmission, pp. 1-1. IET (1990).
[77] M. Barbero, S. Cucchi and M. Stroppiana, "Implementation and performance of an HDTV codec based on the DCT," 1991 IEEE International Symposium on Circuits and Systems (ISCAS), Singapore, 1991, pp. 69-72
[78] L. Cheveau, "The 34 Mbit/s – 8PSK coding system planned for Eurovision," EBU Technical Review (1996).
[79] ETS 300 174: Network Aspects (NA); Digital coding of component television signals for contribution quality applications in the range 34 – 45 Mbit/s ETSI, November 1992.
[80] ITU-T Rec. J.81: "Transmission of component-coded digital television signals for contribution-quality applications at the third hierarchical level of ITU-T Recommendation G.702," International Telecommunication Union, (September 1993).
[81] I. Sebestyén, " Some little-known aspects of the history of the JPEG still picture-coding standard, ITU-T T.81 | ISO/IEC 10918-1 (1986-1993)," ITU Journal: ICT Discoveries, 3(1), (June 2020)
[82] G. Hudson, A. Léger, B. Niss, I. Sebestyén, and J. Vaaben. "JPEG-1 standard 25 years: past, present, and future reasons for a success." Journal of Electronic Imaging 27(4), 040901-040901 (2018).
[83] G.P. Hudson, The European ESPRIT 563 Project, ISO TC97/SC2/WG8 N266, Boston (1986).
[84] G.P., Hudson, D. Tricker, PICA – Photovideotex image compression algorithm, In Directorate General XIII, Telecommunications, Information Industries and Innovation, editor. ESPRIT '86: Results and achievements, pp. 413-422. Amsterdam: North Holland. (1987).
[85] G. P. Hudson, "Photovideotex Image Compression Algorithms-Towards International Standardization." ESPRIT'87 Achievements and Impact. (1987).
[86] H. Yasuda, "Standardization activities on multimedia coding in ISO." Signal processing: image communication, 1(1), 3-16 (1989).
[87] G. P. Hudson, H. Yasuda, and I. Sebestyen, "The international standardization of a still picture compression technique," IEEE Global Telecommunications Conference and Exhibition. Communications for the Information Age, Hollywood, FL, USA, 1016-1021 (1988).
[88] A. Leger, J. L. Mitchell, and Y. Yamazaki, "Still picture compression algorithms evaluated for international standardization," IEEE Global Telecommunications Conference and Exhibition. Communications for the Information Age, Hollywood, FL, USA, 1028-1032 (1988).
[89] D. Le Gall, MPEG: a video compression standard for multimedia applications. Communications ACM 34(4), 46–58 (April 1991).
[90] L. Chairiglione, "Riding the media bits." Online: https://ride.chiariglione.org/ (2011)
[91] ISO/IEC 11172-2, "Information technology — Coding of moving pictures and associated audio for digital storage media at up to about 1,5 Mbit/s — Part 2: Video," ISO and IEC (1993)

[92] ISO/IEC International Standard 13818-2, "Information technology - Generic coding of moving pictures and associated audio information. Part 2: Video," ISO and IEC (November 1994).
[93] ITU-T Recommendation H.262, "Information technology - Generic coding of moving pictures and associated audio information: Video," ITU-T (October 1995).
[94] ITU-T Recommendation H.264, "Advanced video coding for generic audiovisual services," ITU-T, (May 2003).
[95] ISO/IEC 14496-10, "Information technology - Coding of audio-visual objects. Part 10: Advanced Video Coding," ISO and IEC (December 2003).
[96] G. Bjontegaard, "Coding improvement by using 4x4 blocks for motion vectors and transform", ITU-T / Study Group 16 / Question 15, Eibsee, Bavaria, Germany, document Q15-C-23 (December 1997).
[97] ITU-T Recommendation T.832, "Information technology - JPEG XR image coding system - Image coding specification," ITU-T (March 2009).
[98] ISO/IEC 29199-2, "JPEG XR image coding system - Part 2: Image coding specification," ISO and IEC (August 2009).
[99] H. S Malvar, Signal processing with lapped transforms. Artech House, Inc., 1992.
[100] C. Tu, S. Srinivasan, G. J. Sullivan, S. Regunathan, and H. S. Malvar, "Low-complexity hierarchical lapped transform for lossy-to-lossless image coding in JPEG XR / HD Photo," Proc. SPIE 7073, Applications of Digital Image Processing XXXI, 70730C (September 2008).
[101] V. Testoni, M. H. M. Costa, D. Kirovski, and H. S. Malvar. "On the adaptive coefficient scanning of JPEG XR/HD photo," Proc. Data Compression Conference, 69-78 (March 2010),
[102] ITU-T Recommendation H.265, "High efficiency video coding," ITU-T (April 2013).
[103] ISO/IEC ISO/IEC 23008-2, "Information technology - High efficiency coding and media delivery in heterogeneous environments. Part 2: High efficiency video coding," ISO and IEC (December 2013).
[104] A. K. Jain, "A sinusoidal family of unitary transforms," IEEE Trans. Pattern Analysis and Machine Intelligence PAMI-1, 356 –365 (Oct. 1979).
[105] R. K. Chivukula, Y. A. Reznik, "Fast computing of discrete cosine and sine transforms of types VI and VII," Proc. SPIE 8135, Applications of Digital Image Processing XXXIV, 813505 (September 2011).
[106] Y. A. Reznik, "Relationship between DCT-II, DCT-VI, and DST-VII transforms," 2013 IEEE International Conference on Acoustics, Speech and Signal Processing, Vancouver, BC, Canada, 5642-5646 (2013).
[107] J. Han, A. Saxena, and K. Rose, "Towards jointly optimal spatial prediction and adaptive transform in video/image coding," in IEEE Int. Conf. Acoustics, Speech and Signal Processing, Dallas, TX, USA, 726-729 (2010).
[108] A. Saxena, F. C. Fernandes, and Y. A. Reznik, "Fast Transforms for Intra-prediction-based Image and Video Coding," 2013 Data Compression Conference, Snowbird, UT, USA, 13-22 (2013).
[109] J. Sole et al., "Transform Coefficient Coding in HEVC," in IEEE Transactions on Circuits and Systems for Video Technology, 22(12), 1765-1777 (December 2012).
[110] ISO/IEC 23090-3, "Information technology - Coded representation of immersive media. Part 3: Versatile video coding," ISO and IEC (February 2021).
[111] ITU-T Recommendation H.266, "Versatile Video Coding," ITU-T (September 2023).
[112] X. Zhao et al., "Transform Coding in the VVC Standard," in IEEE Transactions on Circuits and Systems for Video Technology, 31(10), 3878-3890 (October 2021).

APPENDIX A. LUKOSZ BOUND AND DISTRIBUTIONS IN FOURIER DOMAIN

Recall that Boas-Kac-Lucosz expression (2) limits the magnitudes of Fourier samples. More specifically, if x, y denote real and imaginary components of a Fourier sample, then it means that $\sqrt{x^2+y^2} \leq \Xi$, where Ξ is some known limit.

If we next model x, y as outputs of a random process, then the same limit must apply to the range (support) of this process. For example, instead of trying to model x, y as outputs of a standard zero-mean Gaussian process:

$$g(x,y) = \mathcal{N}(x|0,\sigma) \cdot \mathcal{N}(y|0,\sigma) = \frac{1}{2\pi\sigma^2} e^{-\frac{x^2+y^2}{2\sigma^2}}, \;\; x,y \in \mathbb{R}, \qquad (A.1)$$

a more appropriate model would be a range-limited Gaussian density:

$$g_{lim}(x,y) = \left(1 - \frac{1}{\sqrt{e^{\xi^2}}}\right)^{-1} \frac{1}{2\pi\sigma^2} e^{-\frac{x^2+y^2}{2\sigma^2}}, \quad x, y \in \mathbb{R}, \sqrt{x^2+y^2} \le \xi\sigma = \Xi\,. \qquad (A.2)$$

Similarly, in the magnitude domain, instead of standard Rayleigh distribution:

$$f(u) = \frac{u}{\sigma^2} e^{-\frac{u^2}{2\sigma^2}}, \quad u \ge 0, \qquad (A.3)$$

a more appropriate model would be a range-limited version:

$$f_{lim}(u) = \left(1 - \frac{1}{\sqrt{e^{\xi^2}}}\right)^{-1} \frac{u}{\sigma^2} e^{-\frac{u^2}{2\sigma^2}}, \quad 0 \le u < \xi\sigma. \qquad (A.4)$$

Let us next understand the *relationship between the range ξ and the variance of the range-limited process $f_{lim}(u)$*. We proceed as follows.

$$\mu_f = \int_0^\infty f(u)u\,du = \sqrt{\frac{\pi}{2}}\,\sigma\,, \qquad \sigma_f^2 = \int_0^\infty f(u)\left(u - \mu_f\right)^2 du = \frac{4-\pi}{2}\,\sigma^2,$$

$$\mu_{lim} = \int_0^\xi f_{lim}(u)u\,du = \left(\sqrt{\frac{\pi}{2}}\operatorname{erf}\left(\frac{\xi}{\sqrt{2}}\right) - \xi e^{-\frac{\xi^2}{2}}\right)\sigma, \qquad \sigma_{lim}^2 = \int_0^\xi f_{lim}(u)(u - \mu_{lim})^2 du =$$

$$= \frac{e^{-\xi^2}}{e^{\frac{\xi}{2}} - 1}\left\{\frac{\pi}{2}\left(e^{\xi^2} + e^{\frac{3\xi^2}{2}}\right)\operatorname{erf}\left(\frac{\xi}{\sqrt{2}}\right)^2 - \xi\sqrt{2\pi}\left(e^{\xi^2} - e^{\frac{\xi^2}{2}}\right)\operatorname{erf}\left(\frac{\xi}{\sqrt{2}}\right) + \xi^2 e^{\frac{\xi^2}{2}} - 2e^{\frac{3\xi^2}{2}} + (\xi^2+1)e^{\xi^2} + \xi^2\right\}\sigma^2.$$

Here σ_{lim}^2 denotes the variance of the range-limited magnitude distribution (A.4), σ_f^2 is the variance of the distribution without the limit (A.3). Figure A.1. presents a plot of the ratio between these two quantities.

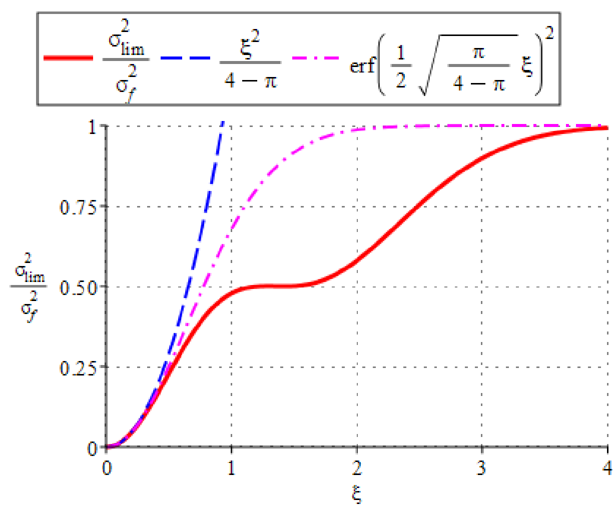

Figure A.1 The effect of the range limit ξ on the variance of magnitude distribution σ_{lim}^2.

As expected, for large ξ we have $\sigma_{lim}^2/\sigma_f^2 \to 1$, and with smaller ξ we observe the decay. The following limits hold:

$$\frac{\sigma_{lim}^2}{\sigma_f^2} \le \operatorname{erf}\left(\frac{1}{2}\sqrt{\frac{\pi}{4-\pi}}\,\xi\right)^2 \le \frac{\xi^2}{4-\pi}.$$